ISSN 0010-9525, Cosmic Research, 2015, Vol. 53, No. 2, pp. 119–127. © Pleiades Publishing, Ltd., 2015.
Original Russian Text © N.S. Nikolaeva, Yu.I. Yermolaev, I.G. Lodkina, 2015, published in Kosmicheskie Issledovaniya, 2015, Vol. 53, No. 2, pp. 126–135.

Modeling of the Corrected D_{st}^* Index Temporal Profile on the Main Phase of the Magnetic Storms Generated by Different Types of Solar Wind

N. S. Nikolaeva, Yu. I. Yermolaev, and I. G. Lodkina

Space Research Institute, Russian Academy of Sciences, ul. Profsoyuznaya, 84/32, Moscow, 117810 Russia
e-mail: nnikolae@iki.rsii.ru

Received May 8, 2014

Abstract—A modeling of the corrected (taking into account the magnetopause currents [9]) D_{st}^* index during the main phase of magnetic storms generated by four types of the solar wind (SW), namely MC (10 storms), CIR (28 storms), Sheath (21 storms), and Ejecta (31 storms), is performed similarly to our previous work on the simple D_{st} index [8]. The "Catalog of large-scale solar wind phenomena during 1976–2000" ([1], ftp://ftp.iki.rssi.ru/pub/omni/) prepared on the basis of the OMNI database, was used for the identification of SW types. The time behavior of D_{st}^* is approximated by a linear dependence on the integral electric field (sumE_y), dynamic pressure (P_d), and fluctuation level (sB) of the interplanetary magnetic field (IMF). Three types of D_{st}^* modeling are performed: (1) by individual values of the approximation coefficients; (2) by approximation coefficients averaged over SW type, and (3) in the same way as in (2) but with allowance for the D_{st}^*-index values preceding the beginning of the main phase of the magnetic storm. The results of modeling the corrected D_{st}^* index are compared to modeling of the usual D_{st} index. In the conditions of a strong statistical scatter of the approximation coefficients, the use of D_{st} instead of D_{st}^* insignificantly influences the accuracy of the modeling and correlation coefficient.

DOI: 10.1134/S0010952515020070

1. INTRODUCTION

This work is dedicated to modeling the temporal profile of the correlated (taking into account magnetopause currents) D_{st}^* index during the main phase of magnetic storms generated by various large-scale types of the solar wind (SW) and is the continuation of a series of publications on study of geomagnetic activity dependence on parameters of the interplanetary space [2–7] and of the process of magnetic-storm generation by various types of SW [8, 9].

Beginning with the publication of Burton et al. [10], it has been shown that D_{st} is well modeled by the SW and IMF parameters. Currently there exist a large number of papers dedicated to the modeling of magnetic storms and their prediction. Various methods are used to predict the D_{st} index, wherein the solar wind–magnetosphere system is considered as a "black box": artificial neuron networks (see, for example, [18–20] and references therein) and nonlinear auto-regression schemes (see, for example, [21, 22] and references therein).

In the majority of papers dedicated to the modeling of geomagnetic storms and their prediction (see, for example, [10, 12, 13, 15, 16]), the type of the SW stream that has generates magnetic storms is not taken into account. At the same time, it is known that different types of SW streams interact with the magnetosphere in different ways (see, for example, [2–7, 9, 11, 20, 23–28]). One recent publication [29] could be used as an example of taking into account the type of solar wind into the forecast of space weather.

In our previous papers [5–9], we looked for a functional relation between storm intensity and interplanetary parameters, and we used the usual geomagnetic index D_{st} for the analysis of development of the magnetic storms main phase and its modeling. However, the D_{st}-index value during magnetic storms is the result of changes in various current systems: the ring current, the current on the magnetopause, and the current of the magnetospheric tail (see, for example, [30–31]). The magnetopause position is governed by an equilibrium between the total pressures in the solar wind and within the magnetosphere. A change in SW dynamic pressure leads to a shift of the magnetopause position to a new equilibrium position. This change is accompanied by both a change in the position of the current sheet on the magnetopause and a change in its value. In order to take into account the contribution of this change in the magnetopause current into the mag-

netospheric D_{st} index, a corrected D_{st}^* index has been proposed which is determined by the formula: $D_{st}^* = D_{st} - b(P_d)^{1/2} + c$, where the coefficients are the following: b is the measure of the response to changes in the SW dynamic pressure (with an increase in the dynamic pressure P_d, the magnetopause approaches the Earth and the contribution of the current related to it is taken into account in D_{st}^*) and c is the measure of the currents on quiet days (see, for example, [10, 12, 13]). Initially the b and c coefficients were taken to be constant and were obtained in [10] for the quiet time using a limited set of SW data. Later the authors [12, 13] obtained new values of these coefficients, to estimate which they used SW data of the OMNI base for a 30-year time period, assuming a possible dependence of the coefficients on interplanetary electric field value ($E_y = VB_s$). For example, the authors showed in [32] that the coefficient b depends on the value of the interplanetary electric field E_y and with its increase (up to $E_y = 18$ mV/m) the value of b decreases by a factor of 5 as compared to the quiet time ($E_y = 0$). However the difference in the values of the coefficient b obtained by various authors using different datasets falls into the 50% scatter of its value in [10, 12, 13, 32].

Using for modeling the corrected D_{st}^* index, we actually take into account the physical process described above and its influence on value of the simple D_{st} index.

In previous publications [8, 9], we took into account the contribution of the SW pressure in the form of the additive term $c_P \cdot P_d$, and it was assumed that the contribution of this term is small (that is, the influence of the SW dynamic pressure on D_{st} is small) and can be approximated by a linear term. The results of [9] showed that for CIR and Ejecta, this term should not be considered small, and the above assumption could be a source of an error. That is why in this paper we process the temporal profile of the corrected (taking into account the magnetopause currents) D_{st}^* index, similar to the correction performed in [9]. The main task of this paper is to obtain an answer to the question: "For which index (D_{st} or D_{st}^*) does our method of modeling the temporal profile of magnetic storm development work better?"

2. INITIAL DATA AND METHOD

In this work we perform a modeling of the temporal profile of the corrected D_{st}^* during the main phase of 90 magnetic storms ($-250 < D_{st} \le -50$ nT) induced by four types of solar wind flows: CIR (28 storms), Sheath (21 storms), MC (10 storms), and Ejectà (31 storms). Because of the absence of data on the corrected D_{st}^*, the number of magnetic storms induced by CIR was slightly reduced as compared to the previous paper [9], but it did not influence the results (see table).

While modeling the main phase of a magnetic storm, a linear approximation of the D_{st}^* index of the main phase of a magnetic storm by three solar wind parameters is used: by the integral of the convective electric field of the solar wind sumE_y, dynamic pressure P_d, and variations in the interplanetary magnetic field sB [9]:

$$D_{st}(i)^* = c_0^* + c_E^* \cdot \mathrm{sum}E_y(i) + c_P^* \cdot P_d(i) + c_B^* \cdot sB(i),$$
$$\mathrm{sum}E_y(i) = \sum_{k=1}^{k=i} E_y(k), \quad (1)$$

where i is the current point of the storm phase which varies from $i = 1$ in the beginning of the phase to $i = im$ at the last point of the storm (in $D_{st\,\min}$), and in sumE_y the summation is performed in terms of k (from the beginning of the storm at point $k = 1$ to the current point of the phase $k = i$). For each type of magnetic storm, the modeling of the main phase is performed in three stages. At first, the individual approximation coefficients $(c_0^*, c_E^*, c_P^*, c_B^*)$ are determined for the main phase of the particular storm of each type. Then the approximation coefficients of the main phase of the storm are averaged over the SW type $\left(\left\langle c_0^* \right\rangle, \left\langle c_E^* \right\rangle, \left\langle c_P^* \right\rangle, \left\langle c_B^* \right\rangle\right)$. At this stage, contributions to the D_{st}^* index of the main phase of particular SW parameters $\left(\left\langle c_E^* \right\rangle \cdot \langle \mathrm{sum}E_y \rangle, \left\langle c_P^* \right\rangle \cdot \left\langle P_d \right\rangle, \left\langle c_B^* \right\rangle \cdot \left\langle sB \right\rangle\right)$ are estimated [9]. At the third stage, corrections taking into account the prehistory of the D_{st}^* index prior to the beginning of the main phase of the magnetic storm are inserted. Instead of the constant average value of the $\left\langle c_0^* \right\rangle$ coefficient, for each storm j (within the given type of SW), the values of $c_0^*(j)$ calculated from the linear dependence of the $c_0^*(j)$ coefficient on the values of the ave$Dst^*(j)$ index, averaged over three points (the point of storm beginning and two preceding points), were taken. The processing method was described in detail in [8, 9].

In order to evaluate the quality of the modeling, we use the linear correlation coefficient (r) and root-mean-square (standard) deviation (σ) between the corrected D_{st}^* and model $D_{st\,\mathrm{mod}}^*$ indices [9].

3. RESULTS

For four types of SW stream (MC, Sheath, CIR, and Ejecta), the table shows the average and median values of the approximation coefficients of the corrected D_{st}^*

Table. Mean and median values of the approximation coefficients and SW parameters (with standard deviations) and also the contributions of these parameters into the D_{st}^{*} (marked by asterisks *) and D_{st} indices during the main phase of magnetic storms for four SW types

SW type	MC 10 storm	Sheath 21 storms	CIR 28/31 storms	Ejecta 31 storms
$\langle c_0^* \rangle$, nT	−32.32 ± 25.6	−28.88 ± 45.1	−38.6 ± 33.7	−40 ± 28
median*	−20	−20	−35.5	−35
$\langle c_0 \rangle$	−13.77 ± 14.4	−13.1 ± 28.8	−28.7 ± 30.5	−30.7 ± 23.1
median	−11	−18	−32	−32
$\langle c_E^* \rangle$, nT V^{-1} m h^{-1}	−2.04 ± 1.1	−3.4 ± 1.9	−2.98 ± 1.5	−2.1 ± 1.1
median*	2	−3	−2.9	−1.7
$\langle c_E \rangle$	−2.55 ± 0.75	−3.2 ± 1.6	−2.82 ± 1.1	−2.3 ± 1.0
median	−2.4	−3.3	−2.8	−2.2
$\langle c_P^* \rangle$, nT/nPa	−0.8 ± 3.5	0.38 ± 3.4	2.72 ± 3.65	1.9 ± 4.5
median*	0	−0.5	2.5	1.6
$\langle c_P \rangle$	−0.92 ± 2.9	0.97 ± 3.3	3.3 ± 3.7	2.8 ± 3.9
median	1	1	2.6	2.8
$\langle c_B^* \rangle$, dimensionless	1.29 ± 3.95	−0.57 ± 2.3	−0.53 ± 2.3	−0.4 ± 2.7
median*	0	−1.3	−0.6	0
$\langle c_B \rangle$	1.28 ± 3.3	−0.8 ± 1.8	−0.19 ± 1.96	−0.2 ± 2.1
median	0	−1	0	0
$\langle \mathrm{sum}E_y^* \rangle$	16.24 ± 9.78	16.4 ± 13.5	13.7 ± 10.7	15.6 ± 11.8
$\langle \mathrm{sum}E_y \rangle$			13.3 ± 10.4	
$\langle c_E^* \rangle \cdot \langle \mathrm{sum}E_y^* \rangle$	−33.12	−55.8	−40.8	−32.8
$\langle c_E \rangle \cdot \langle \mathrm{sum}E_y \rangle$	−41.41	−52.5	−37.5	−35.9
$\langle P_d^* \rangle$	3.62 ± 2.27	5.7 ± 5.7	5.4 ± 3.1	4.3 ± 2.7
$\langle P_d \rangle$			5.5 ± 3.1	
$\langle c_P^* \rangle \cdot \langle P_d^* \rangle$	−2.89	2.16	14.7	8.2
$\langle c_P \rangle \cdot \langle P_d \rangle$	−3.33	5.5	18.15	12.04
$\langle sB^* \rangle$	3.07 ± 2.4	5.1 ± 4.1	5.3 ± 3.3	3.6 ± 2.5
$\langle sB \rangle$			5.4 ± 3.3	
$\langle c_B^* \rangle \cdot \langle sB^* \rangle$	3.96	−2.9	−2.8	−1.44
$\langle c_B \rangle \cdot \langle sB \rangle$	3.93	−4.08	−1.03	−0.72

index of the main phase of magnetic storms ($\langle c_0^* \rangle, \langle c_E^* \rangle, \langle c_P^* \rangle, \langle c_B^* \rangle$ with standard deviations), the average parameters of SW ($\langle \mathrm{sum}E_y^* \rangle$, $\langle P_d^* \rangle$, $\langle sB^* \rangle$ and their standard deviations), and also the contributions of these parameters $\left(\langle c_E^* \rangle \cdot \langle \mathrm{sum}E_y^* \rangle, \langle c_P^* \rangle \cdot \langle P_d^* \rangle, \langle c_B^* \rangle \cdot \langle sB^* \rangle\right)$ to the D_{st}^* index value (these are marked by asterisks *). For the sake of comparison, the table shows also similar parameters for the measured D_{st} index (without asterisks) obtained by us earlier in [9]. For both indices, the mean values of the integral electric field $\langle \mathrm{sum}E_y \rangle$, dynamic pressure $\langle P_d \rangle$, and the level of IMF fluctuations $\langle sB \rangle$ coincide and are not shown in table except for the storms induced by CIR the statistics of which decreased, but the corresponding to them values presented in table are close to each other.

It follows from the table that for D_{st}^* the average value of the $\langle c_0^* \rangle$ coefficient is strongly negative and depends weakly on the type of SW driver of the magnetic storm (the difference is ~38% between the high (negative) value for the Ejecta-induced storms and lower value for the Sheath-induced storms). Depending on the storm type, the value of the $\langle c_E^* \rangle$ coefficient varies within 65% (between the highest (negative) value for the Sheath-induced storms and low value for the storms induced by MC). Taking into account the large scatter of each coefficient for all four SW types, one can see that the $\langle c_E^* \rangle$ coefficients differ substantially depending on the SW type (they are higher for the compression regions CIR and Sheath and lower for MC and Ejecta). The $\langle c_P^* \rangle$ coefficient value is slightly negative for the MC-induced storms, but slightly positive for the other types: Sheath-, CIR-, and Ejecta-induced storms (depending on the SW type, the difference between the positive coefficients $\langle c_P^* \rangle$ reaches a factor of 7 with the minimum and maximum values for the Sheath-induced storms and CIR-induced storms, respectively). One can assume that the $\langle c_P^* \rangle$ coefficient is ~0 for the MC- and Sheath-induced storms, but is high for the CIR- and Ejecta-induced storms (2.7 and 1.9, respectively), but additional studies are needed to increase the significance the result for these types of storms. The value of the $\langle c_B^* \rangle$ coefficient is close to the $\langle c_P^* \rangle$ value, but opposite by sign.

For all types of storms, the integral electric field provides the largest contribution into development of D_{st}^* of the main phase ($\langle c_E^* \rangle \cdot \langle \mathrm{sum}E_y^* \rangle$ in table) with the maximum change (approximately by a factor of 1.7) between the storms induced by Sheath and Ejecta. The contribution of the dynamic pressure $\langle c_P^* \rangle \cdot \langle P_d^* \rangle$ is small for various types of SW (varies between ~3% for Sheath and ~36% for CIR): it changes from a moderate contribution for storms induced by CIR and Ejecta (it weakens the storms) to a small one for storms induced by MC and Sheath (it intensifies the storm by ~10%). The contribution of magnetic fluctuations $\langle c_B^* \rangle \cdot \langle sB^* \rangle$ into development of D_{st}^* is small. For all types of storms it is opposite by sign to the contribution of the dynamic pressure and that leads to their partial compensation for the MC- and Sheath-induced storms (by ~74%) and for CIR- and Ejecta-induced storms (within ~19%).

Figure 1 shows the results of the first stage of modeling of the corrected D_{st}^* index using individual coefficients of approximation of the storm main phase. The correlation coefficients (r) and standard deviations (σ) characterizing the modeling quality are shown in Figs. 4a and 4b. The modeling with individual approximation coefficients (stage one) describes very well D_{st}^* of the main phase for all types of SW. The highest and lowest accuracy of the D_{st}^* modeling is for the MC-induced storms and Sheath-induced storms, respectively (the difference is by a factor of 1.3). For all types of SW, the correlation coefficients are very high (within $r \sim 0.97$–0.99).

Figure 2 shows the results of the second stage of the D_{st}^* modeling, using approximation coefficients averaged over the SW type, so this model can be easily used for real-time forecasting of the storm value, because the coefficients are known in advance [8]. One can see in Figs. 4c and 4d that the accuracy of the D_{st}^* modeling varies approximately by a factor of 1.5 between the highest one for the MC- and Ejecta-induced storms and the lowest one for the Sheath-induced storms, whereas the correlation coefficient is the lowest and highest for the MC- and Shaeth-induced storms, respectively (within $r \sim 0.63$–0.77).

Figures 3, 4e, and 4f show the results of the third stage of the modeling of the main phase D_{st}^* when the model values of $D_{st\,\mathrm{mod}}^*$ are calculated using the approximation coefficients averaged over the SW type (in the same way as at the previous stage 2), taking into account the values of the D_{st}^* index preceding the beginning of the magnetic storm main phase (see [8, 9]). The accuracy of the third stage of the D_{st}^* modeling varies by a factor of ~1.7 from the highest one for the MC-

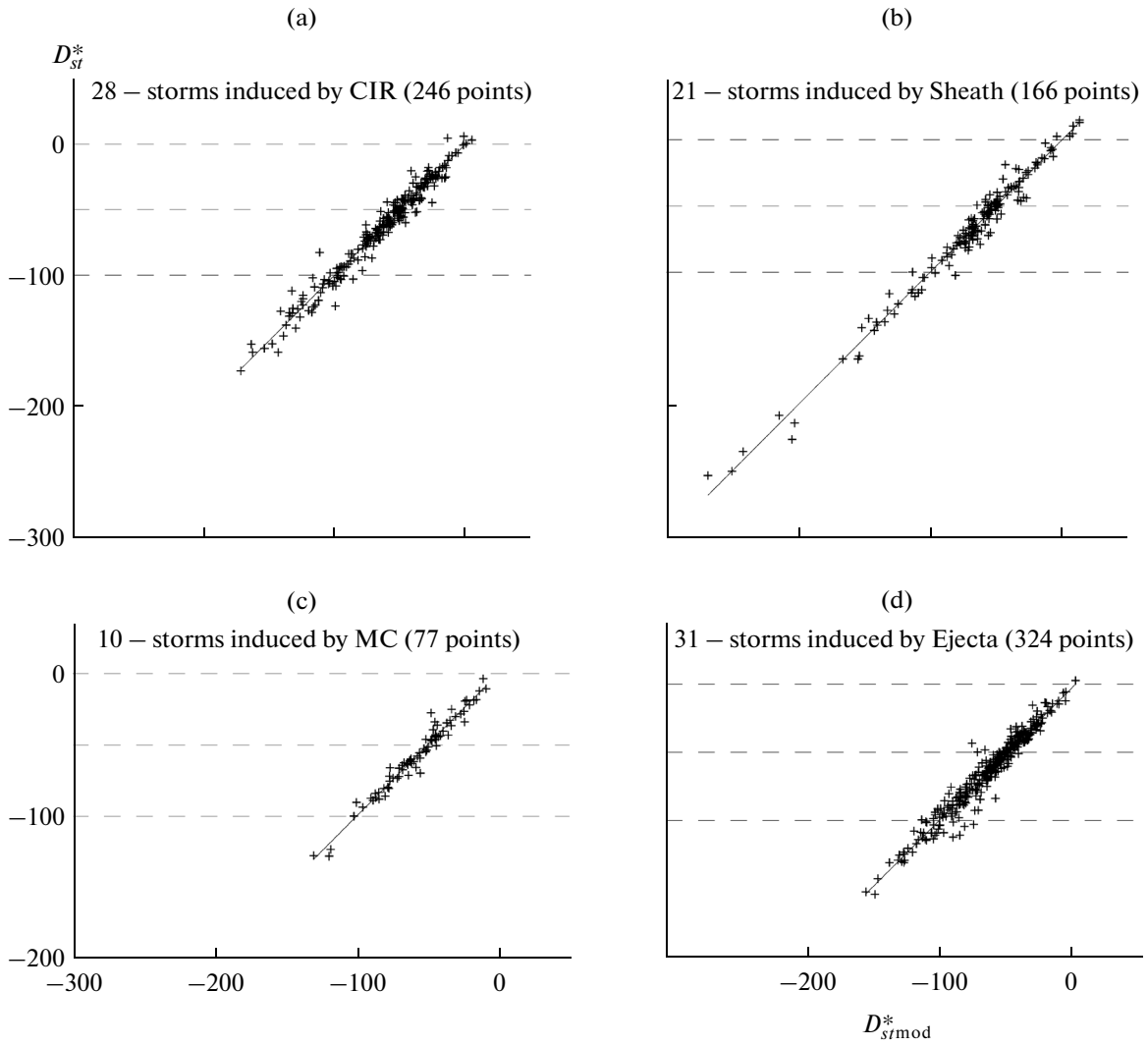

Fig. 1. Dependence of the corrected D_{st}^{*} index on the model value $D_{st\,\mathrm{mod}}^{*}$ with individual approximation coefficients for magnetic storms induced by different SW type (stage 1).

and Ejecta-induced storms to the lowest for the Sheath-induced storms. The correlation coefficient r is high and varies within $r \sim 0.79$–0.82.

4. DISCUSSION AND CONCLUSIONS

The mean values of the approximation coefficients for both the corrected D_{st}^{*} and measured D_{st} indices vary depending on the SW type in a similar way, but insignificantly differ from each other by their value, within the scatter of these coefficients. For all types of SW, the $\left\langle c_0^{*} \right\rangle$ value (as compared to the $\left\langle c_0 \right\rangle$ coefficient) increases ($\left\langle c_0^{*} \right\rangle$ is more negative by a factor of 2.3 and 2.4 for the MC- and Sheath-induced storms, respectively, and by 35 and 33% for the CIR- and Ejecta-induced storms, respectively). For each SW type, the $\left\langle c_E^{*} \right\rangle$ coefficients differ slightly (within 25%) from the $\left\langle c_E \right\rangle$ coefficients. For the Ejecta- and Sheath-induced storms, the $\left\langle c_P^{*} \right\rangle$ coefficient decreased strongly in comparison with $\left\langle c_P \right\rangle$ (by a factor of 1.5–2, still staying positive). The $\left\langle c_B^{*} \right\rangle$ coefficient increased in comparison with $\left\langle c_B \right\rangle$ (became more negative by a factor of 2–2.5) for the Ejecta- and CIR-induced storms, but decreases for the Sheath-induced storms (became less negative by a factor of 1.4), and did not change for the MC-induced storms.

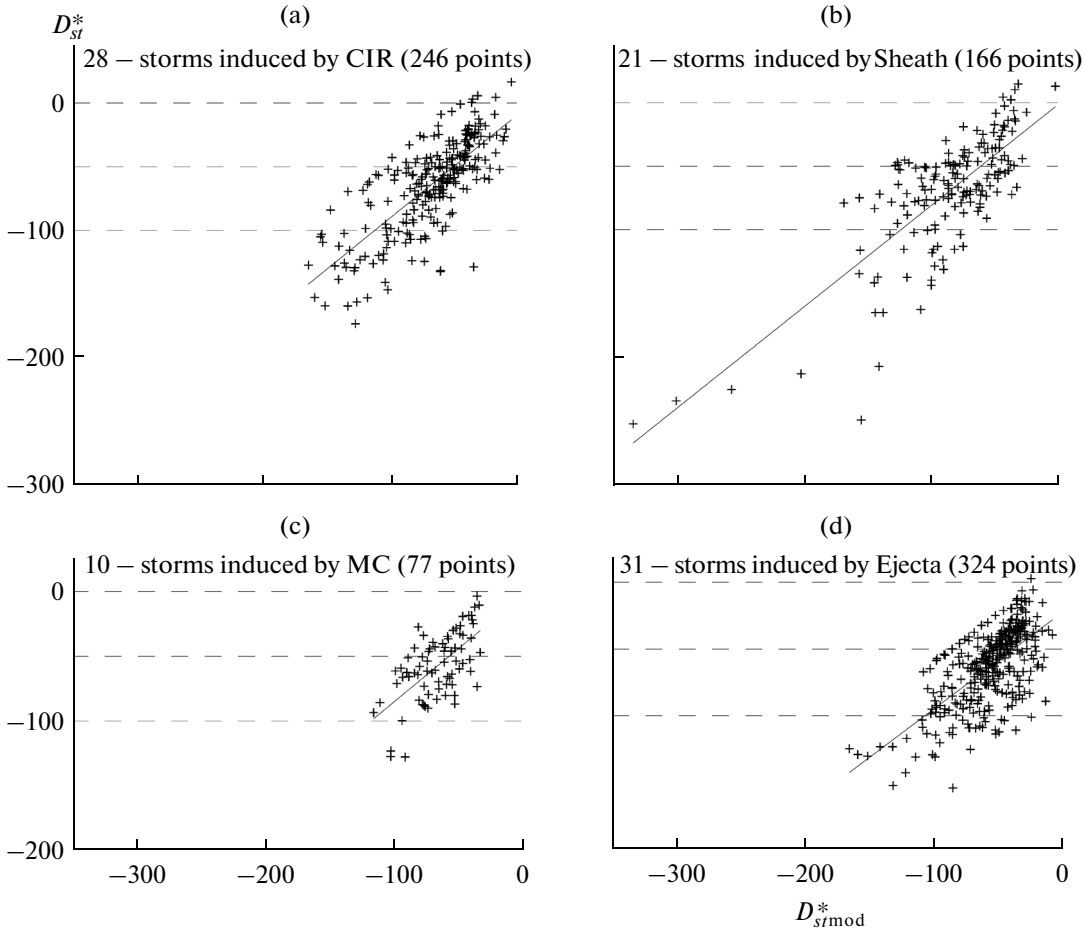

Fig. 2. The same as in Fig. 1, but for $D^*_{st\,\mathrm{mod}}$ with the approximation coefficients averaged over SW types (stage 2).

In comparison with the for the D_{st} index, the contributions of particular parameters into the temporal profile of the corrected D^*_{st} index vary in the following way:

(1) The contribution of the integral electric field $\left\langle c^*_E \right\rangle \cdot \left\langle \mathrm{sum} E^*_y \right\rangle$ changed insignificantly (within 6–32%) for all SW types (staying the largest as compared to other terms of the approximation equilibrium);

(2) The contribution of the dynamic pressure $\left\langle c^*_P \right\rangle \cdot \left\langle P^*_d \right\rangle$ decreased slightly for the MC- and CIR-induced storms (within 15–23%), but became stronger for the Ejecta- and Sheath-induced storms (by a factor of 1.5–2.5);

(3) The contribution of the fluctuations $\left\langle c^*_B \right\rangle \cdot \left\langle sB^* \right\rangle$ increased (in negative value) for the storms induced by Ejecta and CIR by factors of 2 and 2.7, respectively, however a decrease of the contribution from the Sheath-induced storms by 41% (more negative value) is observed. The contributions are the same for the MC-induced storms.

It is important to notice that the formal transition from the D_{st} index to the D^*_{st} index presents an attempt to take into account the contribution into the index of the solar wind pressure via the $b(P_d)^{1/2}$ term, however at approximation by our model, there still remains the dependence of the D^*_{st}-index on the pressure *Pd*: for two types of storms (induced by CIR and Ejecta), the $\left\langle c^*_P \right\rangle$ coefficient does not vanish and the contribution of the pressure $\left\langle c^*_P \right\rangle \cdot \left\langle P^*_d \right\rangle$ still remains substantial (though it decreases). Thus, our results show that in the corrected D^*_{st} index, a dependence on the pressure, possibly, for all SW types (especially for CIR and Ejecta) is present. This fact agrees with the results of other publications [11, 14, 26, 33, 34] demonstrating a rather complicated relation of the D_{st} index to other SW parameters.

At the first stage of the modeling of the corrected D^*_{st} index in comparison with the modeling of the D_{st}, a reduction of modeling accuracy (increase in the standard deviation σ) is typical for all SW types, but is strongest for MC-induced storms (by a factor of ~2).

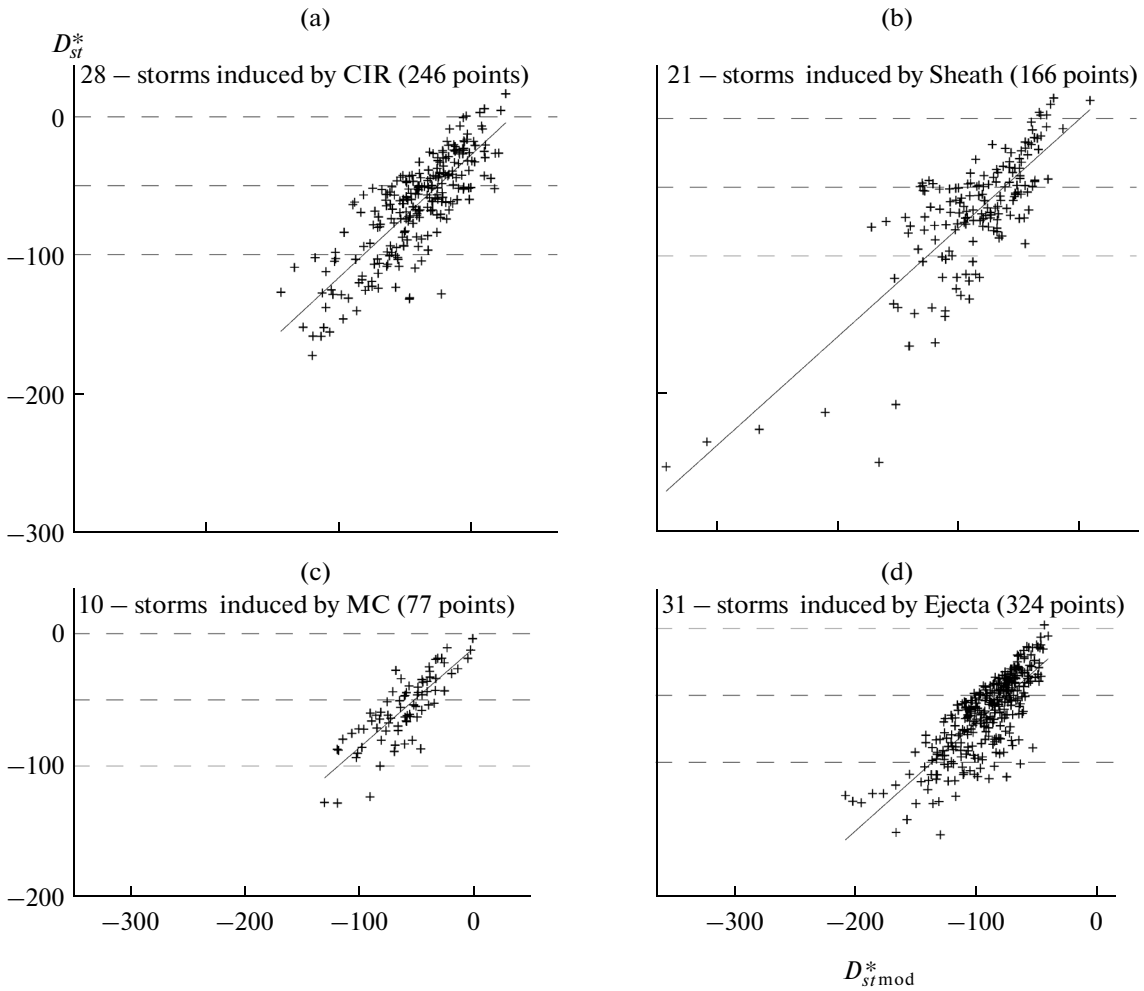

Fig. 3. The same as in Figs. 1 and 2, but for $D_{st\,\mathrm{mod}}^*$ taking into account the D_{st}^*-index values preceding the beginning of the main phase of a magnetic storm (stage 3).

The correlation coefficient values change slightly (within ~1%).

In comparison with the D_{st} index, the second stage of modeling of the corrected D_{st}^* is characterized by a reduction in the accuracy almost for all SW types (within 17–19%) except for the MC-induced storms (an increase by ~3%) and by a decrease in the correlation coefficient for all SW types (within 3–15%), most strongly for Ejecta.

In comparison with the modeling of the D_{st} index, the accuracy of the third stage of modeling of D_{st}^* also decreases for all four SW types (~5–25%), but is stronger for the compression regions CIR and Sheath (19–25%) than for Ejecta and MC (5–9%). The correlation coefficient decreased for all SW types (within ~2–6%), but more strongly for the CIR- and Sheath-induced storms (4–6%) than for the MC- and Ejecta-induced storms (~2%).

It is necessary to emphasize once more that the scatters of the mean approximation coefficients are large enough and, except for $\langle c_E^* \rangle$, exceed substantially their difference between SW types. That is why one can state only tendencies in the differences.

The main conclusions:

(1) Under our method of modeling, the measured D_{st} index describes the dynamics of the main phases of magnetic storms of all SW types at all stages of the modeling more effectively than the corrected D_{st}^* index. It is manifested by higher correlation coefficient r and lower value of σ.

(2) At the second stage of the modeling, the measured D_{st} index describes variations in the main phase of the Ejecta-induced storms better than the corrected D_{st}^* index (that is, provides higher correlation coefficient), but provides a stronger increase in the accuracy (a decrease in the standard deviation σ) of D_{st} (as compared to D_{st}^*) for the Sheath-induced storms.

(3) At the third stage of the modeling (taking into account the index values preceding the beginning of

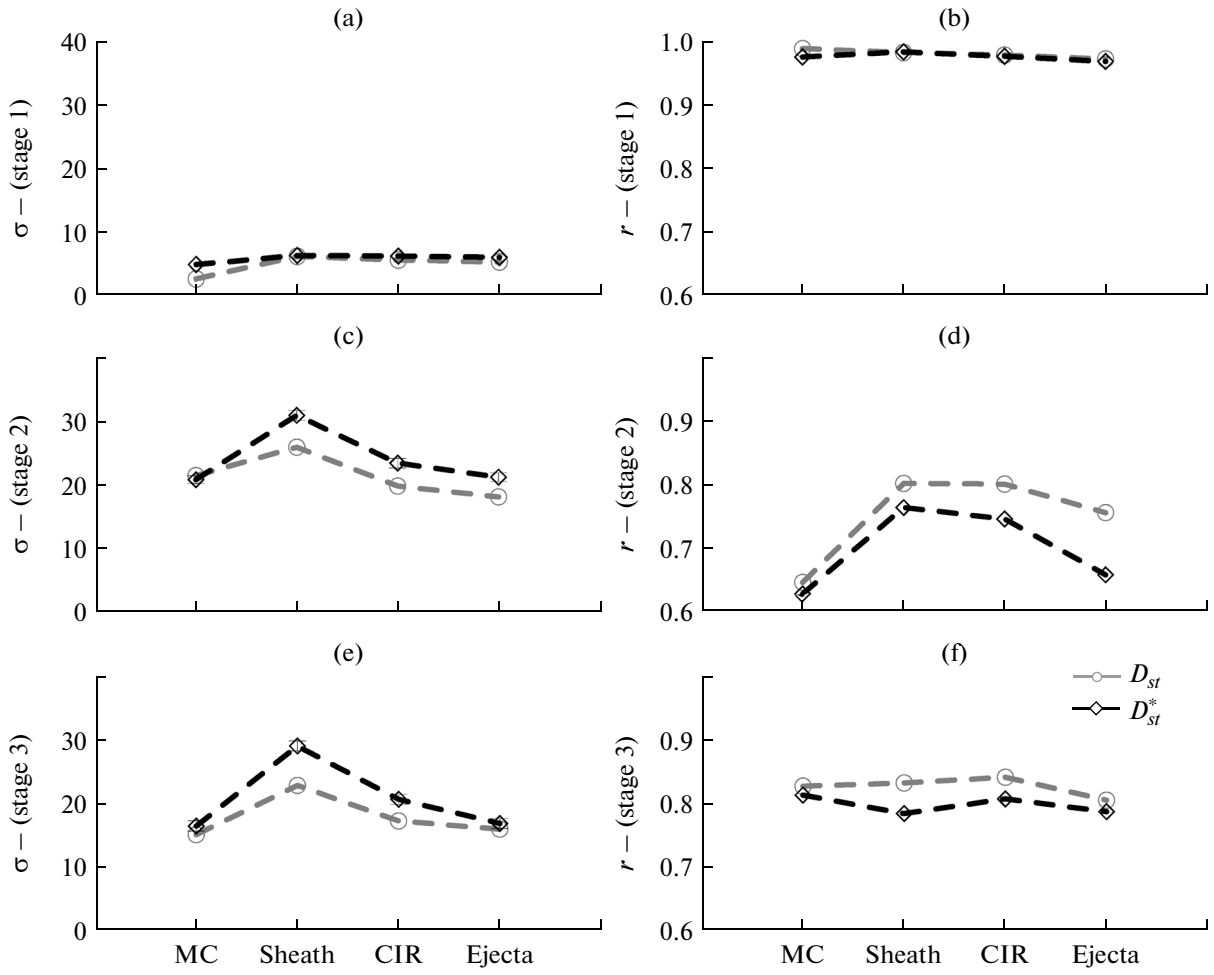

Fig. 4. The standard deviations (σ) and correlation coefficients (*r*) as a function of the SW type at three stages of modeling of main phase: (a, b) by individual coefficients (stage 1), (c, d) by approximation coefficients averaged over SW type (stage 2), and (e, f) taking into account the D^*_{st}-index values preceding beginning of main phase of magnetic storm (stage 3).

the main phase of a magnetic storm), both the D_{st} and D^*_{st} indices describe variations in the main phases of magnetic storms induced by MC and Ejecta almost identically as well (close correlation coefficients and accuracies). At the same time, the CIR- and Sheath-induced storms are better described by the simple D_{st} index than by the corrected D^*_{st} index.

ACKNOWLEDGMENTS

The authors thank for the possibility to use the OMNI database. The OMNI data are obtained from GSFC/SPDF OMNIWeb at the site http://omniweb.gsfc.nasa.gov. The work was supported by Russian Foundation for Basic Research (project no. 13-02-00158a) and also by the Program of the Presidium of RAS (no. P22).

REFERENCES

1. Yermolaev, Yu.I., Nikolaeva, N.S., Lodkina, I.G., and Yermolaev, M.Yu., Catalog of large-scale solar wind phenomena during 1976–2000, *Kosm. Issled.*, 2009, vol. 47, no. 2, pp. 99–113. [*Cosmic Research*, pp. 81–94].
2. Yermolaev, Yu.I., Lodkina, I.G., Nikolaeva, N.S., and Yermolaev, M.Yu., Statistical study of interplanetary condition effect on geomagnetic storms, *Kosm. Issled.*, 2010, vol. 48, no. 6, pp. 499–515. [*Cosmic Research*, pp. 485–500].
3. Yermolaev, Yu.I., Lodkina, I.G., Nikolaeva, N.S., and Yermolaev, M.Yu., Statistical study of interplanetary condition effect on geomagnetic storms: 2. Variations of parameters, *Kosm. Issled.*, 2011, vol. 49, no. 1, pp. 24–37. [*Cosmic Research*, pp. 21–34].
4. Yermolaev, Yu.I., Nikolaeva, N.S., Lodkina, I.G., and Yermolaev, M.Yu., Specific interplanetary conditions for CIR-, Sheath-, and ICME-induced geomagnetic storms obtained by double superposed epoch analysis, *Ann. Geophys.*, 2010, vol. 28, pp. 2177–2186.

5. Nikolaeva, N.S., Yermolaev, Yu.I., and Lodkina, I.G., Dependence of Geomagnetic Activity during Magnetic Storms on the Solar Wind Parameters for Different Types of Streams, *Geomagn. Aeron.*, 2011, vol. 51, no. 1, pp. 51–67.
6. Nikolaeva, N.S., Yermolaev, Yu.I., and Lodkina, I.G., Dependence of Geomagnetic Activity during Magnetic Storms on the Solar Wind Parameters for Different Types of Streams: 2. Main Phase of Storm, *Geomagn. Aeron.*, 2012, vol. 52, no. 1, pp. 28–36.
7. Nikolaeva, N.S., Yermolaev, Yu.I., and Lodkina, I.G., Dependence of Geomagnetic Activity during Magnetic Storms on the Solar Wind Parameters for Different Types of Streams: 3. Development of storm *Geomagn. Aeron.*, 2012, vol. 52, no. 1, pp. 37–48.
8. Nikolaeva, N.S., Yermolaev, Yu.I., and Lodkina, I.G., Dependence of Geomagnetic Activity during Magnetic Storms on the Solar Wind Parameters for Different Types of Streams: 4. Simulation for Magnetic Clouds, *Geomagn. Aeron.*, 2014, vol. 54, no. 2, p. 152–161.
9. Nikolaeva, N.S., Yermolaev, Yu.I., and Lodkina, I.G., Modeling the time behavior of the D_{st} index during the main phase of magnetic storms generated by various types of solar wind, *Kosm. Issled.*, 2013, vol. 51, no. 6, pp. 443–454. [*Cosmic Research*, pp. 401–412].
10. Burton, R.K., McPherron, R.L., and Russell, C.T., An empirical relationship between interplanetary conditions and Dst, *J. Geophys. Res.*, 1975, vol. 80, pp. 4204–4214.
11. Fenrich, F.R. and Luhmann, J.G., Geomagnetic response to magnetic clouds of different polarity, *Geophys. Res. Lett.*, 1998, vol. 25, pp. 2999–3002.
12. O'Brien, T.P. and McPherron, R.L., An empirical phase space analysis of ring current dynamics: Solar wind control of injection and decay, *J. Geophys. Res.*, 2000, vol. 105, pp. 7707–7720.
13. O'Brien, T.P. and McPherron, R.L., Forecasting the ring current index Dst in real time, *J. Atmos. Solar-Terr. Phys.*, 2000, vol. 62, pp. 1295–1299.
14. Wang, C.B., Chao, J.K., and Lin, C.-H., Influence of the solar wind dynamic pressure on the decay and injection of the ring current, *J. Geophys. Res.*, 2003, vol. 108, no. A9, p. 1341. doi: 10.1029/2003JA009851.
15. Siscoe, G., McPherron, R.L., Liemohn, M.W., Ridley, A.J., and Lu, G., Reconciling prediction algorithms for Dst, *J. Geophys. Res.*, 2005, vol. 110, A02215. doi: 10.1029/2004JA010465.
16. Podladchikova, T.V. and Petrukovich, A.A., Extended geomagnetic storm forecast ahead of available solar wind measurements, *Space Weather*, 2012, vol. 10, S07001. doi: 10.1029/2012SW000786.
17. Vassiliadis, D., Klimas, A., and Baker, D., Models of Dst geomagnetic activity and of its coupling to solar wind parameters, *Phys. Chem. Earth*, 1999, vol. 24, pp. 107–112. doi: 10.1016/S1464-1917(98)00016-6.
18. Wu, J.-G. and Lundstedt, H., Geomagnetic storm predictions from solar wind data with the use of dynamic neural networks, *J. Geophys. Res.*, 1997, vol. 102, pp. 14255–14268. doi: 10.1029/97JA00975.
19. Lundstedt, H., Gleisner, H., and Wintoft, P., Operational forecasts of the geomagnetic Dst index, *Geophys. Res. Lett.*, 2002, vol. 29, no. 24, p. 2181. doi: 10.1029/2002GL016151.
20. Barkhatov, N.A., Levitin, A.E., and Revunov, S.E., Complex classification of global geomagnetic disturbances, *Cosmic Research*, 2006, vol. 44, no. 6, pp. 468–478.
21. Balikhin, M.A., Boynton, R.J., Billings, S.A., Gedalin, M., Ganushkina, N., Coca, D., and Wei. H., Data based quest for solar wind–magnetosphere coupling function, *Geophys. Res. Lett.*, 2010, vol. 37, p. L24107. doi: 10.1029/2010GL045733.
22. Boynton, R.J., Balikhin, M.A., Billings, S.A., and Amariutei, O.A., Application of nonlinear autoregressive moving average exogenous input models to geospace: Advances in understanding and space weather forecasts, *Ann. Geophys.*, 2013, vol. 31, pp. 1579–1589.
23. Borovsky, J.E. and Denton, M.H., Differences between CME-driven storms and CIR-driven storms, *J. Geophys. Res.*, 2006, vol. 111, A07S08. doi: 10.1029/2005JA011447.
24. Denton, M.H., Borovsky, J.E., Skoug, R.M., Thomsen, M.F., Lavraud, B., Henderson, M.G., McPherron, R.L., Zhang, J.C., and Liemohn, M.W., Geomagnetic storms driven by ICME and CIR-dominated solar wind, *J. Geophys. Res.*, 2006, vol. 111, A07S07. doi: 10.1029/2005JA011436.
25. Pulkkinen, T.I., Partamies, N., Huttunen, K.E.J., Reeves, G.D., and Koskinen, H.E.J., Differences in geomagnetic storms driven by magnetic clouds and ICME sheath regions, *Geophys. Res. Lett.*, 2007, vol. 34, p. L02105. doi: 10.1029/2006GL027775.
26. Turner, N.E., Cramer, W.D., Earles, S.K., and Emery, B.A., Geoefficiency and energy partitioning in CIR-driven and CME-driven storms, *J. Atmosph. Sol.-Terrest. Phys.*, 2009, vol. 71, pp. 1023–1031.
27. Despirak, I.V., Lubchich, A.A., and Guineva, V., Development of substorm bulges during storms of different interplanetary origins, *J. Atmosph. and Sol.-Terrest. Phys.*, 2011, vol. 73, pp. 1460–1464.
28. Yermolaev, Y.I., Nikolaeva, N.S., Lodkina, I.G., and Yermolaev, M.Yu., Geoeffectiveness and efficiency of CIR, Sheath, and ICME in generation of magnetic storms, *J. Geophys. Res.*, 2012, vol. 117, p. A00L07. doi: 10.1029/2011JA017139.
29. Barkhatov, N.A., Levitin, A.E., and Revunova, E.A., Classification of space weather complexes based on solar source type, characteristics of plasma flow, and geomagnetic perturbations induced by it, *Geomagn. Aeron.*, 2014, vol. 54, no. 2, p. 173.
30. Tsyganenko, N.A., Sitnov, M.L., Modeling the dynamics of the inner magnetosphere during strong geomagnetic storms, *J. Geophys. Res.*, 2005, vol. 110, A03208. doi: 10.1029/2004JA010798.
31. Levitin, A.E., Dremukhina, L.A., Gromova, L.I., and Ptitsyna, N.G., Modeling giant disturbances of the geomagnetic field,, in *"Physics of Auroral Phenomena." Proc. XXXIV Annual Seminar. Apatity,* 2011, pp. 29–32.
32. Siscoe, G.L., McPherron, R.L., and Jordanova, V.K., Diminished contribution of ram pressure to Dst during magnetic storms, *J. Geophys. Res.*, 2005, vol. 110, A12227. doi: 10.1029/2005JA011120.
33. O'Brien, T.P. and McPherron, R.L., Evidence against an independent solar wind density driver of the terrestrial ring current, *Geophys. Res. Lett.*, 2000, vol. 27, pp. 3797– 3799.
34. Asikainen, T., Maliniemi, V., and Mursula, K., Modeling the contributions of ring, tail, and magnetopause currents to the corrected Dst index, *J. Geophys. Res.*, 2010, vol. 115, A12203. doi: 10.1029/2010JA015774.

Translated by A. Danilov